2024 33rd IEEE International Conference on
Robot and Human Interactive Communication (RO-MAN)
August 26-30, 2024. Pasadena, California, USA.

2024 33rd IEEE International Conference on Robot and Human Interactive Communication (ROMAN) | 979-8-3503-7502-2/24/$31.00 ©2024 IEEE | DOI: 10.1109/RO-MAN60168.2024.10731263

On Experimental Energy Consumption Estimation of a 6-DoF Industrial UR3e Robot Arm Manipulator in Trajectory Planning

Sara Hosseini, IEEE Student Member
University of Erlangen-Nuremberg (FAU)

Institute of Electrical Drives and Machines
Erlangen, Germany
sara.hosseini@fau.de

Ingo Hahn, Senior Member, IEEE
University of Erlangen-Nuremberg (FAU)

Institute of Electrical Drives and Machines
Erlangen, Germany
ingo.hahn@fau.de

***Abstract*— This paper proposes an energy consumption estimation in the trajectory planning task of an industrial robot (IR) arm manipulator. Human-robot collaborative scheduling has become integral to modern manufacturing. Effective scheduling of human-robot cooperation is crucial for enhancing production efficiency. However, energy-efficient trajectory planning in human-robot interaction remains an unexplored area. To address this, a 6-DoF (Degree of Freedom) robot arm, available in the laboratory, was utilized to assess the energy consumption of this specific robot type. However, his approach can be applied to any robot, whether it's a human-robot collaboration, a mobile robot, or any other articulated robot arm manipulator.**

For this goal the electrical and mechanical losses of a 6-DoF robot arm manipulator from the company *Universal Robots* is modeled and its power losses cost function (PLCF) is derived correspondingly to calculate the electromechanical energy losses. The objective of this paper is to estimate the energy losses in a trajectory planning task in cartesian space for a tool center point (TCP) of the robot, starting from an initial point and resting at a final point. This goal is achieved by examining and analyzing the kinematics and dynamics followed by measuring the velocity and acceleration related terms of each motor at each joint of the UR3e robot arm in a laboratory setup. The results estimate the changes of energy losses in the overall trajectory following of the robot manipulator and presents the results of the estimated and measured reduction terms.

K*eywords—power consumption, industrial robot, motion planning, electromechanical losses, six degree of freedom robot*

I. INTRODUCTION

In the mechatronic industry, industrial robots (IR) as well as in daily lives the Human-Robots are getting more attention day by day and IRs are crucial as the primary components of automated manufacturing systems, especially for handling and material processing tasks. The decision to incorporate IR is primarily driven by the robot's exceptional attributes of repeatability, accuracy, speed, and efficiency [1]. Utilizing IR in manufacturing systems not only enables industries to slash operating costs but also enhances productivity. However, among stringent CO2 emissions policies and escalating energy expenses, there's a pressing need to curtail the energy consumption of IRs [2]-[4]. Notably, IRs' energy usage constitutes roughly 8% of the total electrical energy used in manufacturing processes. [5]. Therefore, it is crucial to lower energy consumption to ensure the efficiency of manufacturing systems. Additionally, exploring the energy consumption of robots through research can help manufacturers develop strategies to tackle new production challenges. For example, the increasing use of renewable energy sources creates a need for flexible energy supply, requiring proactive approaches [6]. As a result, reducing the energy consumption of robots in daily lives not only supports sustainability goals but also prepares industries to adjust to changing energy dynamics in manufacturing. In the year 2022 an estimated amount of 3.903.633 IRs was in operation worldwide due to international federation of robotics [7]. From which solely in 2022, 545.000 units were installed worldwide which is around 5% more installations than in the previous year 2021 with 519.000 newly installed units. This shows the increase of the automated industries in the modern world. From which just in Germany the electronic industries were largest costumers of robotics in 2022 and gained the first ranked position of energy consumption which was 28%, the automotive industry followed with 25% of the installations and metal and machinery industry at third place with 12% installations. Followed by fourth place plastics and chemical products with 4% and food and beverage with 3% of the overall installations of IRs [8], [9].

Trajectory planning for IRs encompasses various approaches, including time-optimal trajectory planning [10]-[12], shortest path methods like straight-line and ant colony algorithms [13], and time-extension techniques [14]. Additionally, other optimal trajectory planning objectives are considered, such as those focused on energy efficiency.

Hence the first step to estimate the energy losses of the robot is to model the power losses. This is different for each type of robot while each robot has its unique kinematic and dynamic model. In this paper the model of a power loss cost function (PLCF) for the industrial robot from the universal robot (UR3e) is attained regarding its electrical and mechanical losses. Then these losses are evaluated regarding different trajectory scenarios. The simulated and measured results are then presented to validate the gained and estimated energy losses during a given task of trajectory following of the robot.

In the remainder of this paper, we present in Section II the kinematic and dynamic model of the UR3e robot arm. This is the first step toward an energy model of an IR and will enable the development of energy optimal process planning. In Section III we will develop the power losses cost function of this robot followed by Section IV which gives the overview of the architecture of the experimental laboratory system setup and how the robot is connected to the controller and host, and how the connection with different connection interface protocols is done. In Section V the trajectory interpolation method is introduced followed by an experimental investigation which is carried out to measure and estimate the energy losses of the trajectory planning task such as pick and place, electronics assembling tasks in the production of the company or durable welding tasks. Finally, a conclusion and outlook to further work will be given in Section VI.

II. The Kinematics and Dynamics Model of the UR3e Robot

The dynamic model of a robot arm connects the actuator torques to the manipulator's motion profiles. This model includes various kinematic parameters like joint positions and orientations, along with dynamic parameters such as masses, center-of-mass positions, and inertia components. The following sections, A and B, will present the kinematic and dynamic models of the UR3e.

A. Kinematics of the UR3e

In order to derive the forward dynamics model for a robot manipulator to get the torque of each joint and hence model the PLCF, it is imperative to first establish a forward kinematic model. For this goal the model of the robot and its Denavit-Hartenberg (DH) parameters should be introduced. Fig. 1.a illustrates the visual schematic model of the UR3e robot. The kinematic model is derived using the DH convention and the kinematic parameters are listed in Table I. Additionally, Fig. 1.b depicts the DH reference frames of the UR3e. If we define $\Lambda(.)$ as a transformation from the robot's joint angles $\theta = (\theta_1, \theta_2, \theta_3, \theta_4, \theta_5, \theta_6)$ to the TCP (tool center point) of the robot, the forward kinematics (FK) will be achieved. On the other hand, the inverse kinematics (IK) is involved with transforming the pose of the TCP in cartesian space $p = (x, y, z, o_x, o_y, o_z)$ to the joint angles, where x, y, z are the position parameters in cartesian 3D space and o_x, o_y, o_z are the orientation parameters of the TCP. Therefore, the FK will be as

$$p = \Lambda(\theta) \tag{1}$$

and IK as

$$\theta = \Lambda^{-1}(p) \tag{2}$$

where θ describes the joint angle vector of frames.

TABLE I. D-H Parameters of UR3e Robot Arm

Joint	$\alpha\ [rad]$	$d\ [m]$	$\theta\ [rad]$	$a\ [m]$
1	0	0.1519	0	$\pi/2$
2	-0.24365	0	0	0
3	-0.21325	0	0	0
4	0	0.11235	0	$\pi/2$
5	0	0.08535	0	$-\pi/2$
6	0	0.0819	0	0

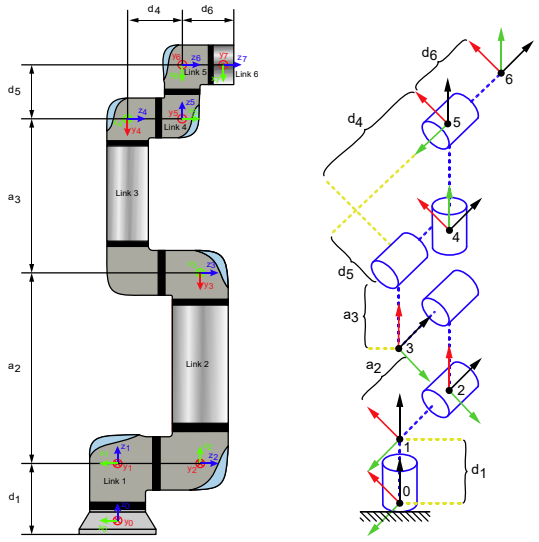

(a) Visual model (b) DH reference frames

Fig. 1: Schematic of the *Universal robot UR3e* robot arm

B. Dynamics of the UR3e

The UR3e robot's equations of motion adhere to a comprehensive rigid-body dynamic model depicted as

$$D_{n\times n}(\theta)\ddot{\theta}_{n\times 1} + H_{n\times n}(\theta, \dot{\theta})\dot{\theta}_{n\times 1} + G_{n\times 1}(\theta) = \tau_{n\times 1} \tag{3}$$

As the IR has 6 joints therefore, $D(\theta)$ represents a (6×6) inertia and mass dependent matrix, $H(\theta, \dot{\theta})$ denotes a (6×6) Coriolis and centrifugal matrix, $G(\theta)$ signifies a (6×1) gravity vector, and τ symbolizes a (6×1) generalized torque vector encapsulating joint torques effects. Notably, this generalized model operates within joint space, capturing the entirety of the robot's behavior solely through the angular displacements of its joints. In (3) the vector $\theta = [\theta_1\theta_2\theta_3\theta_4\theta_5\theta_6]^T$ is the vector of joint angles and $\dot{\theta}$ and $\ddot{\theta}$ are the (1×6) vectors of angular velocity and acceleration.

III. Energy Losses Estimation

In order to derive the power losses cost function (PLCF) for the complete PTP (Point-to-Point) motion for an industrial robot task such as electronic assembly in the production line of the factories, Welding robots or servant robots at the shopping centers, it is essential to incorporate both the electromechanical model of the motors along with the entire 6-DoF (Degrees of Freedom) manipulator system.

Each joint of the UR3 robot arm manipulator consists of a PMSM motor. Considering the voltage drop across the motor as below contributes for all the joints of the robot

$$V_n(t) = R_n I_n(t) + L_n \frac{dI_n(t)}{dt} + k_{e_n}\dot{\theta}_n \tag{4}$$

In this context, k_{e_n} denotes the diagonal matrix representing the back-electromotive force (EMF) constant, R_n stands for the winding resistance, and L_n signifies the inductance pertaining to the n^{th} motor. The instantaneous electrical power P_e drawn by the robot is consequently succinctly articulated through the voltage-current product as illustrated below:

$$P_e(t) = V(t)^T I(t) \quad (5)$$

Conversely the terminal currents of each join of the robot and the torques of each join of the robot τ_n, are related through the diagonal matrix of each motor's torques constant, as shown in equation (6):

$$\tau_n = k_{t_n} I_n(t) \quad (6)$$

Upon substituting equation (4) into equation (5), the instantaneous power drawn by each joint of the robot is subsequently expressed as equation (7), wherein the impact of the inductors on power absorption is disregarded:

$$P_e(t) = R_n I_n^2(t) + k_{e_n} \dot{\theta}_n(t) I_n(t) \quad (7)$$

On the contrary, to get the mechanical related losses from (6), the current at each motor is gained which is dependent on torque and torque constant of each joint. Substituting this $I_n(t) = \frac{\tau_n}{k_{t_n}}$ current into the equation (7) and knowing the τ_n is as (3), the electromechanical power losses cost function ($PLCF_{EM}$) which contributes to the electrical losses as well as mechanical losses, will be as gained as in (8) [15]. Nevertheless in [15] the PLCF is developed for a 2DoF robot arm manipulator, however what makes this model engaging is that this model is based on the fact that can be extended to 6DoF or even higher orders of DoF of robots.

$$PLCF_{EM}(\theta, \dot{\theta}, \ddot{\theta}, t) = \ddot{\theta}^T A(\theta)\ddot{\theta} + \ddot{\theta}^T B(\theta)\dot{\theta} + \dot{\theta}^T C(\theta)\dot{\theta} + d(\theta)\ddot{\theta} + e(\theta)\dot{\theta} + f(\theta) \quad (8)$$

In (8) the PLCF is dependent on the sum of constant matrices namely A, B, C, d, e, f, associated with angular position of the robot at each instant, its velocity and acceleration and their products and squared values. Where $A(\theta), B(\theta)$ and $C(\theta)$ are 6×6 matrices and $d(\theta), e(\theta)$ and $f(\theta)$ are 1×6 vectors which are dependent to the parameters as in equations (9) to (15) and Table II.

$$A(\theta) = R_a . K . D(\theta)^T . D(\theta) \quad (9)$$

$$B(\theta) = \left(R_a . K . V_f(\theta) + k_e k_t^{-1}\right) D(\theta) \quad (10)$$

$$C(\theta) = \left(R_a . K . V_f^T(\theta) + k_e k_t^{-1}\right) V_f(\theta) \quad (11)$$

$$d(\theta) = R_a . K . D(\theta) G(\theta) \quad (12)$$

$$e(\theta) = (R_a . K . D(\theta) + k_e^{-1} k_t^{-1}) G(\theta) \quad (13)$$

$$f(\theta) = G(\theta)^T . R_a . K . G(\theta) \quad (14)$$

$$K = (k_t k_e^T)^{-1} \quad (15)$$

By means of integrating (8) over a time interval of the predefined task of the robot namely $[t_i, t_f]$, where t_i denotes the initial time and t_f denotes the final resting time of the motion, and then adding up the all PLCFs of all joints in this time interval for the 6-DoF of UR3e in real time and in joint space, the overall energy loss W_{EM} is estimated as:

$$W_{EM} = \int_{t_i}^{t_f} \sum_{k=1}^{n} PLCF_{EM}\, dt \quad (16)$$

where n denotes the number of the joints.

TABLE II. COEFFICIENT PARAMETERS OF THE PLC

Parameter	Description of the matrix
$\boldsymbol{D(\theta)}$	Inertia and Mass
$\boldsymbol{R_a}$ $\boldsymbol{[\Omega]}$	Winding resistance
$\boldsymbol{k_t[Nm/A]}$	Torque constant
$\boldsymbol{k_e[V.sec/degree]}$	Back-emf constant
$\boldsymbol{G(\theta)}$	Gravity force
$\boldsymbol{V_f(\theta)}$	Viscous friction

IV. OVERVIEW OF EXPERIMENTAL SYSTEM SETUP ARCHITECTURE

The experimental setup comprises a personal computer (PC) and a Universal Robots (UR3e) robot, consisting of three primary components: robot arm, control box, and teach pendant, as depicted in Fig. 2. The input data of the robot's registers to follow the desired trajectory profile are logged through the Polyscope (teach pendant), which features a graphical touch interface or as an alternative via the PC using a TCP/IP connection from MATLAB® client which in this experimental measurement the TCP/IP Connection is used. Data logging is managed by a Python client via RTDE protocol. The controller executes user-provided high-level programs and transmits commands for the robot arm's execution. Conversely, the robot arm relays information back to the controller. This information is utilized by the controller, for example, to assess whether the robot should proceed with its task or halt in the event of unexpected occurrences.

The robot arm embodies a sophisticated 6 degree-of-freedom (DOF) serial-link articulated robot manipulator configuration, wherein the robot's links are arranged sequentially, enabling rotary motion at the joints. Each joint integrates an electric actuator, precisely a three-phase Permanent Magnet Synchronous Machine (PMSM), alongside a strain-wave transmission mechanism. The PMSM efficiently transmits high-velocity/low-torque power to the input axle, while the transmission system subsequently converts this power to low-velocity/high-torque output at the axle.

V. TRAJECTORY PLANNING AND SIMULATIONS

The trajectory interpolation method which is used in this paper is the 5th order polynomial as shown in (17) in cartesian space which guarantees the 6 boundary conditions of position,

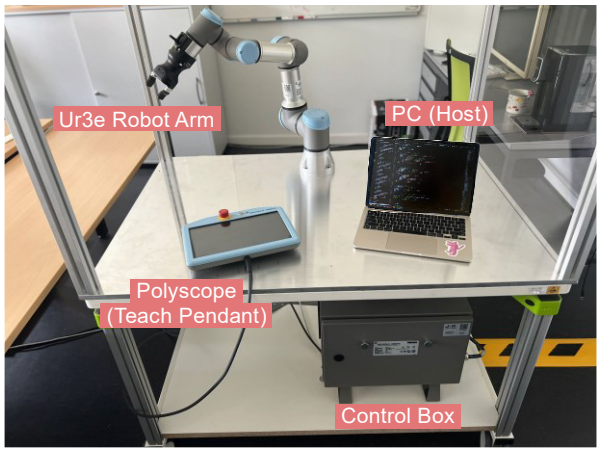

Fig. 2: Architecture of the testbench setup

velocity and acceleration at the beginning of the motion and at the final resting time instant of it.

$$x(t) = a_0 + a_1 t + a_2 t^2 + a_3 t^3 + a_4 t^4 + a_5 t^5 \qquad (17)$$

Choosing a higher order namely a 7th order polynomial fulfills the position, velocity and acceleration boundary condition, however on the other side results in higher overshoots of the motion which is unnecessary. Choosing a lower order of polynomial as 3rd order, will not fulfil the boundary conditions of specifying the initial and final accelerations. Accordingly in the 3D motion of the TCP of the UR3e in cartesian space, the same interpolation is implemented for the $y(t)$ and $z(t)$ axis to assure the same criteria of motion boundary conditions for initial and final time instants. It is desired that the TCP of the robot starts in cartesian space from the initial pose coordinates of

$$p = [88.55, -336.81, -5.53, 1.39, -2.96, 0.14]$$

and rests at the same point. The first 3 elements of vector p denote the position (x, y, z) coordinates of TCP in Cartesian space and the last 3 elements denotes its Euler orientation (o_x, o_y, o_z) elements. To this aim, two scenarios of circular trajectories of the TCP are to be investigated to be able to estimate the energy losses during the whole operation task. The first circular movement of the TCP has the radius of 35 cm whereas the second one has the radius of 75 cm and the overall time to estimate the energy losses is 8s as illustrated in Fig 3. To be able to implement the trajectory planning to the registers of the robot, the *ur_rtde* module of the Python library has been installed on the Windows-based computer operator and the *Control* and *Receive* modules are used to make connection between client and host. The data is transferred

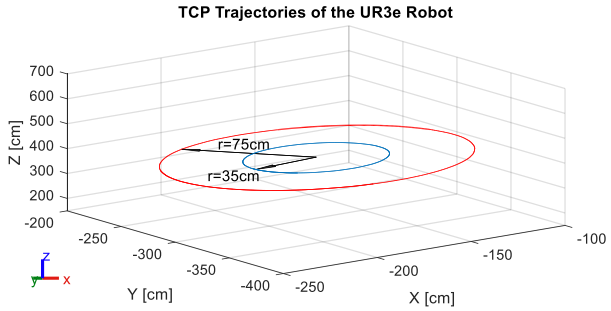

Fig. 3: Circular Trajectories of TCP for radii of 35cm and 75cm

with the frequency of 500 Hz to the robot joints. The desired trajectory is then given to the TCP of the robot in cartesian space and the desired and measured values of angular velocity in $°/s$ and acceleration in $°/s^2$ of the robot motors are measured and recorded for each joint in the total interval of 8 seconds through the controller at the PC. The results can be seen in the Fig. 4 and Fig 5. As in (8) and (16) the energy losses of any type of robot depends vigorously on the angular velocities and accelerations of the 6 motors. Independent of which type of robot is used, either it is a Articulated Robot, a Autonomus Mobile Robot, Humanoid or Cobots, the energy losses of each robot depends on these two motion profile scenarioss. The only difference is the electrical and mechanial constants and their corresponding topology model. Yet in general, their dependency on the motion profiles is the strong reason to analyse the motion profiles to be able to get an energy-efficient trajectory planning for any type of robot. Fig. 4 (a) and (b) show the angular velocity for both scenarios of

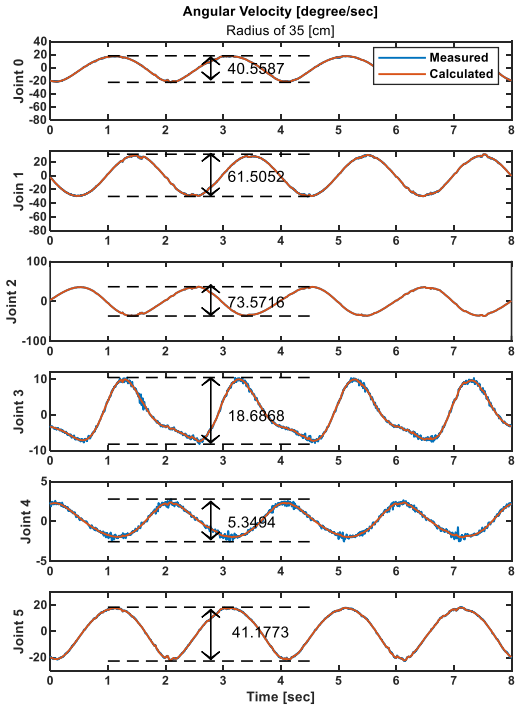

(a) First scenario with the radius of 35 cm

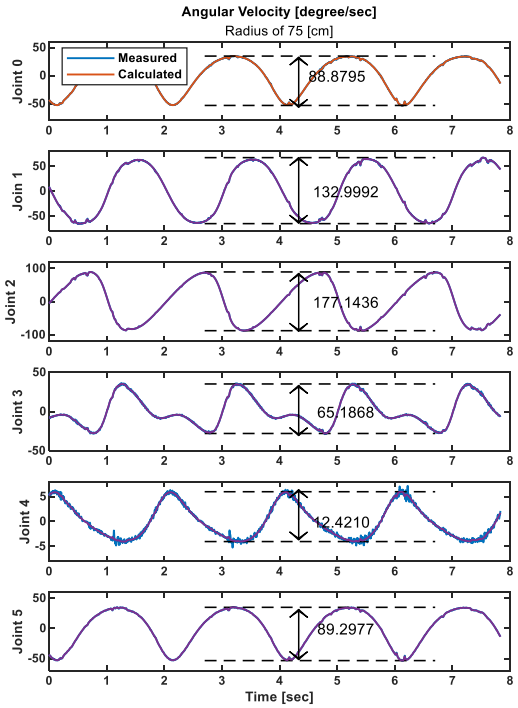

(b) Second scenario with the radius of 75 cm

Fig. 4: Measured angular velocities of 6 joints

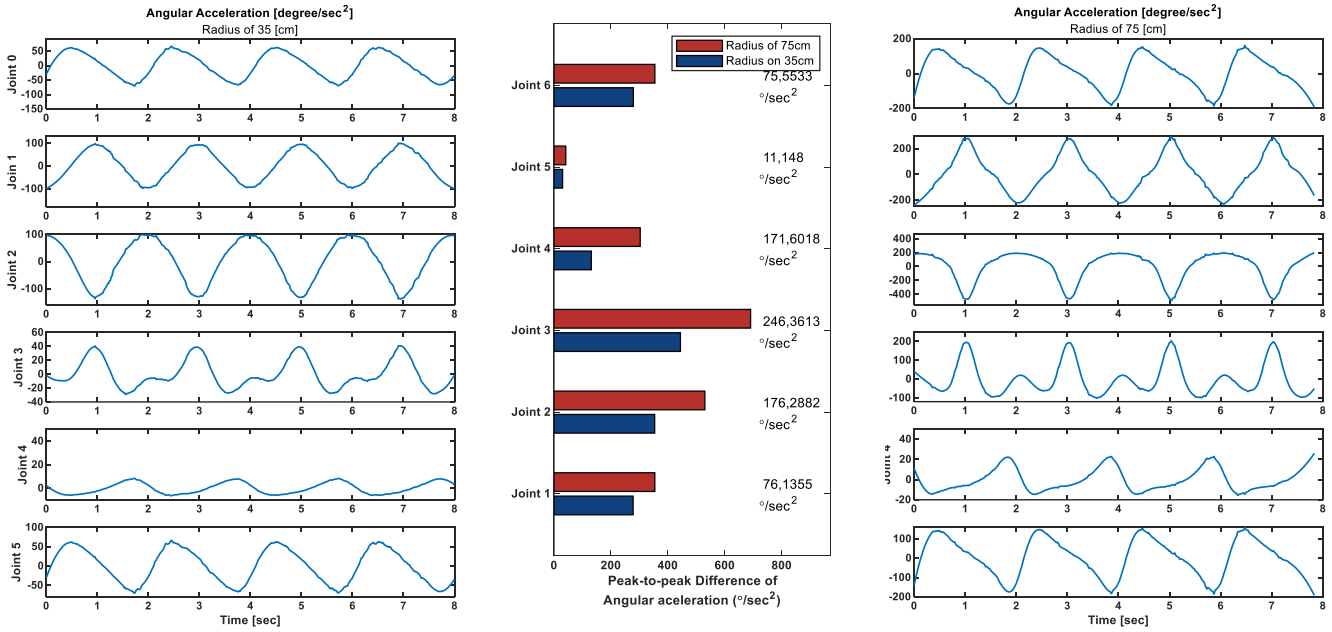

(a) (b) (c)

Fig. 5: (a) Measured acceleration profiles for all 6 motor joints' or the UR3e robot for the task of fist scenario (b) The comparison between the reduced peak-to-peack acceleration fo both scenarios (c) Measure acceleration profiles for all 6 motor joints' or the UR3e robot for the task of second scenario

the trajectory with the radius of 35 cm and 75 cm respectively from left to right. For every joint the peak-to-peak angular velocity is measured and shown in the figure. Comparing the maximum and minimum values of the velocity for the first motor in the base frame, it could be seen that the peak-to-peak amount of the first scenario with the radius of 35 cm which is $40.5587\,°/s$, has roughly 45% less velocity changes in comparison to the angular velocity of it's peer of the 2nd scenario with $88.8795\,°/s$.

Looking closely to the peak-to-peak velocities of the 2nd, 3rd , …, 6th motor peers in Fig. 3 it could be concluded that the peak-to-peak value of the velocity for motor peers 1 to 6, is reduced by 53%, 59%, 72%, 58% and 53% from scenario 2 to 1. Therefore the velocity related terms in (18) will also decrease with an average of 56% in total.

$$W_{EM} = \int_{t_i}^{t_f} \sum_{k=1}^{n} \begin{matrix} \ddot{\theta}^T A(\theta)\ddot{\theta} + \ddot{\theta}^T B(\theta)\dot{\theta} + \\ \dot{\theta}^T C(\theta)\dot{\theta} + d(\theta)\ddot{\theta} + e(\theta)\dot{\theta} + f(\theta) \end{matrix} dt \qquad (18)$$

The same also is extendable for the acceleration terms of the PLCF in (18) to estimate the reduction of acceleration related losses in the two already mentioned scenarios. As seen in Fig 4.a the measured results of angular acceleration of all 6 motors of the robot arm for the first scenario with the radius of 35 cm show less peak-to-peak oscillations in comparison to Fig. 5.c for the second scenario with 75 cm. As depicted in Fig 4.b the bar diagram concludes the reduction of peak-to-peak angular acceleration, this reduction for the 1st to 6th joints' motor peers are: $76.1355\,°/s^2$, $176.2882\,°/s^2$, $246.3613\,°/s^2$, $171.6018\,°/s^2$, $11.148\,°/s^2$, $75.5533\,°/s^2$ respectively. This yields that the peak-to-peak reduction of the acceleration profiles from scenario 2 to scenario 1 is reduced by 23%, 33%, 35%, 56%, 26% and 21% for the 1nd to 6th jonts' motor peers respectively. The average of acceleration related terms' reduction in the (18) is estimated to have an average of 32%.

VI. Conclusion

This paper introduces an energy-efficient trajectory planning approach utilizing a proposed electrical power loss model. The objective is to determine optimal motion profiles to estimate the energy consumption for human-robot by testing the results on an robot arm. To achieve this, a UR3e robot arm manipulator with PMSM motor types is employed in the experimental setup. Considering various factors such as electrical winding resistance losses, mechanical losses including inertia, Coriolis and centrifugal forces, friction, and gravitational terms, real-time torque data for each joint of the UR3e is collected over a period of 8 seconds. Subsequently, the Power Loss Cost Function (PLCF) of the manipulator is derived and proposed incorporating the mentioned electromechanical factors. Two trajectory scenarios, generated using a circular movement in Cartesian space with 5th order polynomial interpolation method, are then analyzed to observe the effects of changes in angular velocities and accelerations on the PLCF. The findings are presented through simulation and measurement, and and it has been demonstrated that reducing the peak-to-peak velocities leading to smoother motion profiles by a certain amount results in a significantly reduction of the energy consumption of the trajectory planning task. This is because the PLCF factors depend on the velocity and acceleration terms solely, their product and their squared terms. In future work, numerical optimization algorithms will be employed to identify the most energy-efficient trajectory between two points. Regarding the gained results, it is proved that whith

optimising the acceleration of deceleration of the motors in the joints of any type of robot it is possible to find an energy efficient motion. This leads to more sustainablity of the robot itself aswell as saving energy and costs.

REFERENCES

[1] Chettibi E, Lehtihet HE, Haddada M, Hanchi S (2004) "Minimum cost trajectory planning for industrial robots". Eur J Mech A-Solid 23:703–715

[2] Franke J, Kreitlein S, Risch F, Guenther S (2013) "Energy effficient production strategies and technologies for electrical drives". IEEE International Conference on Industrial Technology (ICIT)

[3] Thiede S (2012) "Energy efficiency in manufacturing systems". Springer, Berlin Heidelberg

[4] Bornschlegl M, Drechsel M, Kreitlein S, Franke J (2014) "Holistic approach to reducing CO2 emissions along the energy-chain (E-chain)". In: Wellnitz, et al. (eds) Sustainable automotive technologies 2013. Lecture Notes in Mobility 2014, pp 227-234

[5] Engelmann J (2009) „Methoden und Werkzeuge zur Planung und Gestaltung energieeffizienter Fabriken". Dessertation, TU Chemnitz

[6] Popp R, Keller F, Atabay D et al (2013) „Technische innovationen fur die Energieflexible Fabrik". ZWF 108(7–8):556–560

[7] Wrold Robotics, Industrial Robots 2023

[8] HERRMANN, C.; THIEDE, S.: Process chain simulation to foster energy efficiency in manufacturing. In: CIRP Journal of Manufacturing Science and Technology 1, 4 (2009), pp. 221–229

[9] BMWi: Zahlen und Fakten Energiedaten: Struktur des Energieverbrauchs, Deutschland. 2014-03-03

[10] ZHANG Lei, et al.Modeling and trajectory planning of four-DOF robot grasping moving target[J]. Manufacturing Automation, 2017,39(12):44—48

[11] LIU Peng,et al.Research on Trajectory Planning and Simulation of Motorman up50 Robot[J]. Machine Building & Automation, 2016, 45(03): 162-164+226

[12] SHAO Yuanyuan, XUAN Guantao, LIU Jing, HOU Jialin. Reverse-driving trajectory planning of welding robot with NURBS[J]. THANSACTIONS OF THE CHINA WELDING INSTITUTION, 2014, 35(6): 9-12

[13] Shen Junwei,Cheng Heng.Trajectory Planning Optimization of Two-degree-of-freedom Parallel Mechanism[J].Journal of Mechanical Transmission. 2021,45(07):110—115.

[14] S. Hosseini und I. Hahn, "Energy-Efficient Motion Planning for Electrical Drives", IEEE Electrical Power and Energy Conference (EPEC), Toronto, ON, Canada, 2018.

[15] S. Hosseini und I. Hahn, "Kinodynamic Motion Planning and energy Loss Cost Function Modelling for a 2-DOF Robot Arm Manipulator", IEEE Electrical Power and Energy Conference (ICIT), Buenos Aires, Argentina 2020